NANO LETTERS

2008
Vol. 8, No. 4
1105-1110

Biofunctionalized Lipid−Polymer Hybrid Nanocontainers with Controlled Permeability

Alma Dudia,*,†,|| Armağan Koçer,‡,§ Vinod Subramaniam,† and Johannes S. Kanger*,†

Biophysical Engineering, BMTI Institute for Biomedical Technology and MESA+ Institute for Nanotechnology, Faculty of Science and Technology, University of Twente, P.O. Box 217, 7500 AE Enschede, The Netherlands, and BioMaDe Technology Foundation, Nijenborgh 4, 9747 AG, Groningen, The Netherlands

Received December 9, 2007; Revised Manuscript Received February 8, 2008

ABSTRACT

We have successfully developed, for the first time, a novel polymer–lipid hybrid nanocontainer with controlled permeability functionality. The nanocontainer is made by nanofabricating holes with desired dimensions in an impermeable polymer scaffold by focused ion beam drilling and sealing them with lipid bilayers containing remote-controlled pore-forming channel proteins. This system allows exchange of solutions only after channel activation at will to form temporary pores in the container. Potential applications are foreseen in bionanosensors, nanoreactors, nanomedicine, and triggered delivery.

The development of single molecule imaging techniques in recent years has made it possible to follow biochemical reactions at the level of individual molecules and obtain information that is often hidden by ensemble averaging in bulk measurements (for a recent review see ref 1). One of the requirements of single molecule techniques is the ability to follow an individual molecule for sufficiently long times in solution. However, it is a challenge to cope with the effects of Brownian motion on this time scale. To meet this challenge, more recently, biomolecules have been encapsulated inside lipid vesicles,[2] which are themselves tethered to the surface. Vesicles serve as a biologically relevant environment, where reactions occur in small compartments, and it provides freedom to the molecules, as long as they are not interacting with the vesicle walls. The major disadvantage of vesicle encapsulation, on the other hand, is the difficulty to exchange the substances/solutions between the interior and the exterior of the vesicles due to the lipid bilayer barrier. Cisse et al. solved this problem by generating porous lipid nanocontainers by incorporating a channel protein, α-hemolysin, which introduces permanent pores into synthetic lipid vesicles and enables exchange with the bulk solution.[3] Alternatively, Broz et al. designed nanocontainers from polymers for stability and equipped them with yet another channel protein, OmpF, which allows the passive diffusion of polar molecules and equilibration of internal and external solutions.[4] Unfortunately, these two approaches provide no control over the permeability; the channel pores are permanently open so that ions or small molecules are exchanging constantly. Additionally, in the latter case, the polymer wall thickness critically influences the activity of many other alternative channel proteins. Here, for the first time, by combining the advantages of both lipid and polymer containers, we have generated an advanced biohybrid nanocontainer. It is composed of a polymer vesicle with a lipid membrane patch covering a nanohole fabricated in the vesicle wall (Figure 1). The lipid membrane patch itself contains an engineered channel protein designed to allow for the passage of molecules up to a diameter of 3 nm.[5] This system offers the controlled communication between the interior and exterior of the vesicle containers, which is desirable for single molecule imaging, and a very important property for micro- to nanodevices and for delivery of drugs or imaging agents in vitro and in vivo.

The scaffold of the hybrid nanocontainer is made of a polymer for stability, biocompatibility, and tunable physi-

* Corresponding authors: e-mail alma.dudia@gmail.com, tel +31503635523, fax +31503634429; e-mail J.S.Kanger@utwente.nl, tel +31534893726, fax +31534891105.

† University of Twente.

‡ BioMaDe Technology Foundation.

|| Present address: BioMaDe Technology Foundation.

§ Present address: Department of Biochemistry, Groningen Biomolecular Sciences and Biotechnology Institute & Zernike Institute for Advanced Materials, University of Groningen, Nijenborgh 4, 9747 AG, Groningen, The Netherlands.

10.1021/nl073211b CCC: $40.75
Published on Web 03/01/2008

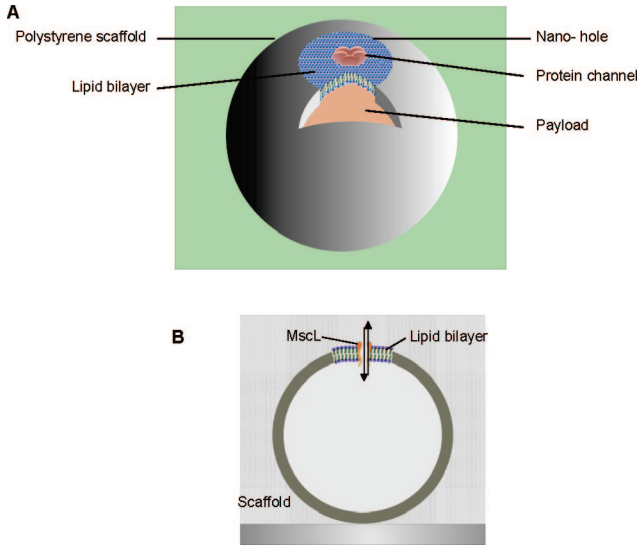

Figure 1. (A) Schematic representation of a hybrid nanocontainer, consisting of an impermeable hollow polymeric scaffold with a single small opening and a payload inside the scaffold. Synthetic bilayer lipid membrane with embedded MscL channels seals the hole. (B) Cross section of the hybrid nanocontainer. Typical dimensions of this structure are approximately 1 μm in diameter, wall thickness ~100 nm, and hole dimension is in the submicrometer range.

cochemical properties such as toughness, surface charge, hydrophilicity, degradation kinetics, permeability, and temporal stability.[6] In this work polystyrene was used as the polymer scaffold. The polymer wall separates the inner compartment of the nanocontainer from the external environment, in analogy with the compartmentalization functionality of a real biological membrane.

In order to enhance the flexibility of the system for incorporation of biomolecules without impeding their function, a lipid membrane patch was sealed over a hole in the scaffold. The hole dimensions were designed such that their submicrometer diameters lent stability to the membrane. It has been previously shown that membranes spanning smaller holes exhibit a longer temporal stability and are less susceptible to breakage due to mechanical disturbance, vibrations, and surface tension.[7–9]

The last component of the system is a remote-controlled channel protein, which is reconstituted in the lipid patch before sealing the hole. It allows the loading and unloading of a payload at a desired time and/or location. The channel protein chosen is the mechanosensitive channel of large conductance (MscL) from *Escherichia coli*.[10] In nature, MscL works as a safety valve. Under severe hypoosmotic stress conditions, it responds to tension in the membrane by undergoing structural changes and forming a temporary pore in the membrane.[11] The open MscL pore has a diameter of about 3 nm and allows the passage of not only ions and small molecules but also small proteins.[5,12] Even though MscL is a mechanosensitive channel, random mutagenesis experiments showed that insertion of a charged or polar amino acid or chemical compounds into the hydrophobic pore region of the channel can elicit opening of the pore in the absence of tension.[13,14] Recently, the charge formation and, thus, channel opening could be influenced in a controlled manner such that the channel opening could be actuated at will externally by light, ambient pH, or combinations of these effectors.[15–17]

In order to obtain the hybrid device, we first fabricated nanoholes with defined dimensions in the hollow polymer scaffolds (hollow polystyrene beads, Polysciences, Warrington, PA). Single holes in the scaffolds with an outer diameter of ~1 μm and wall thickness of 100 nm were made by focused ion beam (FIB) drilling.[18] FIB drilling is a maskless and fast method for etching and imaging with nanometer resolution and has traditionally been used for etching conductive materials.[19] FIB has been applied previously for etching of nanocavities in colloidal particles to achieve an optical cavity inside a photonic crystal[20] and for accessing the cross sections of latex particles for scanning electron microscopy imaging and analysis.[21] These approaches have required surface modifications to avoid building up of ionic charge during FIB processing. However, we have been able to make single holes with defined diameters on hollow polymer scaffolds by applying FIB without any modifications of the surface properties of the polystyrene scaffolds. To achieve this result, the scaffolds were supported on a metal holder to minimize charge buildup during FIB processing (see methods in the Supporting Information). An image of a polystyrene scaffold into which a single hole was etched using a 1.5 pA gallium ion current is shown in Figure 2A. The time required to etch a hole with dimensions of 200 nm $\times$ 200 nm through the 100 nm thick polystyrene wall is approximately 12 s. The etching is controllable with respect to the number of holes and the dimensions of the hole. Furthermore, the scaffold maintains its position on the support, despite the local ionic charging of the polystyrene surface that occurs during the etching. The effect of the FIB etching on the structure of the scaffold was explored by removing one-half of the scaffold (using FIB etching with the same current for about 90 s) and imaging the scaffold at an angle, as shown in Figure 2B. Clearly, the scaffold remained hollow and the hole existed only on the top of the scaffold, as intended, with no additional structural damage to the scaffold. It was also possible to fabricate polystyrene scaffolds with two holes without damaging the integrity of the structure (see Figure S1 in the Supporting Information).

We obtained full control over the hole diameter by exploring the relation between the hole surface area and the required etching time for a given etching current. Figure 3 shows the required etching time as a function of the surface area of a single square hole for a FIB current of 1.5 pA. The etching time increased with increasing the hole surface area in a linear manner with a correlation coefficient of ~0.99. However, this linear relation does not hold for hole sizes with a diameter less than 100 nm (Figure 3, inset). In these cases, the hole dimension is smaller than the wall thickness of the scaffold and therefore the redeposition rate of the etched material is strongly increased,[18,19] resulting in a longer etching time.

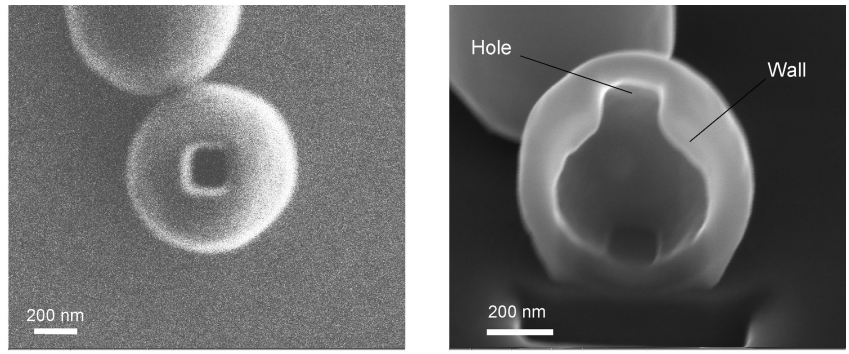

Figure 2. (A) FIB image of a dried scaffold (outer diameter of 0.83 μm, wall thickness of 100 nm) containing a single hole of 200 nm × 200 nm. The hole was etched using a current of 1.5 pA. (B) FIB image of the scaffold with a hole (see A) rotated under an angle, where half of the scaffold was etched away using a current of 9 pA.

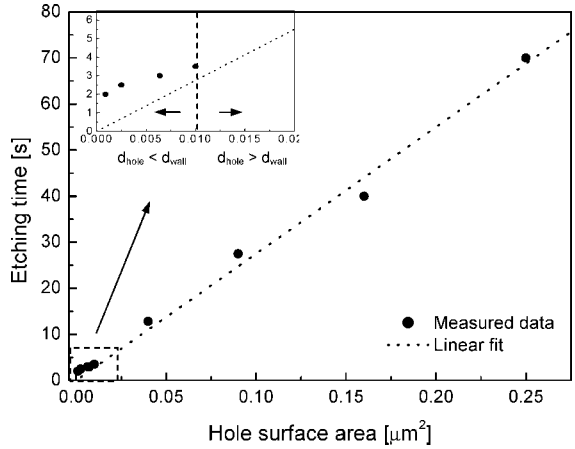

Figure 3. Time required for etching single square holes as function of the hole surface area: (●) Data obtained with FEI FIB Nova 600 nano laboratory using a minimum etching current of 1.5 pA. Dotted line gives a linear fit of the data. The inset shows a zoom in at small hole surface areas. The vertical dashed line represents the boundary where diameter of the hole (d_{hole}) is equal to the thickness of the scaffold wall (d_{wall}).

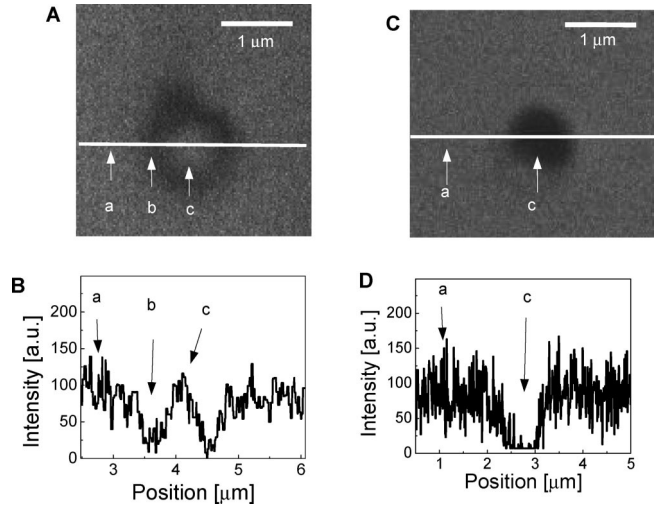

Figure 4. Characterization of scaffold loading: (A) CLSM image through the center of a scaffold filled with aqueous solution of Rhodamine 123 containing ethanol; (C) a scaffold with no hole, immersed in 2% ethanol-Rhodamine 123 solution. (B) and (D) present the fluorescence intensity cross-sectional line profiles across the lines as indicated in images (A) and (C), respectively. a, b, and c denote the bulk medium, scaffold wall, and scaffold interior, respectively. It should be noted that the dimensions of the scaffold are close to the optical resolution of the microscope, which prevents observation of sharp transitions between the nonfluorescent wall and the fluorescent solution.

We achieved high scaffold fabrication yields (~90% of all attempts were successful). On average, about 20 min was required to manually select ~15–20 single scaffolds, to focus on their surface, and to drill single holes in those scaffolds.

In order to show the loading of the polymer scaffolds through the engineered bare nanohole, we used confocal laser scanning microscopy (CLSM). To this end, hydrophobic polystyrene scaffolds containing single nanoholes were loaded with aqueous solution of fluorescent dye (Rhodamine 123, concentration of 39.4 μM) in the presence of 2% (v/v) of ethanol.[22] Ethanol was used to reduce the surface tension occurring at the region of the nanohole, thereby facilitating the loading of the scaffold. We recorded the fluorescence intensity distributions from a confocal slice close to the center of a scaffold. Figure 4A depicts the fluorescence image of a scaffold loaded with aqueous Rhodamine 123 solution. Loading occurred within a few seconds after immersing the dried scaffolds in the dye solution. A fluorescence intensity profile clearly indicated that the scaffold was filled with dye (Figure 4B). The loading yield was 100% for the hole-containing scaffolds. The control scaffolds without any holes, on the other hand, did not give any fluorescence signal under the same conditions, indicating the impermeability of the scaffold to the fluorescent dye (see panels C and D of Figure 4).

Toward the external control over the permeability of the fabricated nanocontainer, as a first step, the holes were sealed with a synthetic lipid bilayer by the controlled collapse of unilamellar giant vesicles (GUVs) onto the holes (see Materials and Methods in the Supporting Information). First, the scaffold surface was positively charged by incubation with 0.01% poly-L-lysine in phosphate buffered saline (PBS, pH 7.4). To facilitate electrostatic interaction with the liposomes, negatively charged GUVs were prepared from 1,2-diphytanoyl-*sn*-glycero-3-phosphocholine, 1-palmitoyl-2-oleoyl-*sn*-glycero-3-[phospho-*rac*-(1-glycerol)], and cholesterol (ratio 70:25:5 wt %) in the presence of 400 mM

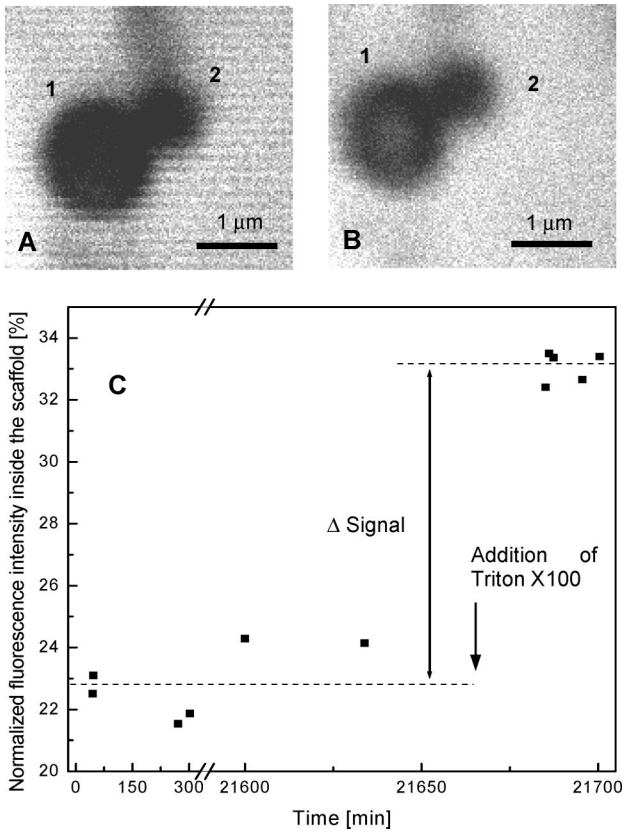

Figure 5. (A) CLSM image of a nanofabricated (1) and a control (2) scaffold. A single hole (300 nm × 300 nm) was covered with the lipid membrane, both scaffolds immersed in buffer−calcein solution. (B) Scaffolds in (A) after addition of 7 mM Triton X100. (C) Normalized fluorescence intensity inside the sealed scaffold prior to and after Triton X100 addition. Fluorescence intensity is normalized to the bulk intensity. The arrow indicates the time of Triton X100 addition in the bulk solution for rupturing the membrane. Prior to membrane deposition, the medium was refreshed with ethanol-free buffer.

glucose with repeated freeze and thaw cycles. Then, GUVs were fluorescently labeled with [4-(4-(dihexadecylamino)styryl)]-*N*-methylpyridinium iodide, DiA. Individual single GUVs were trapped with optical tweezers (output laser power ∼0.2 W) and maneuvered to the hole in the scaffolds. Their collapse was initiated by physical contact with the scaffold surface. This procedure takes, on average, 2−5 min to complete. The membrane deposition was monitored in real time by epifluorescence microscopy. A fluorescent dye, calcein, was added to the bulk solution to a final concentration of 0.5 mM in order to probe the quality of the sealing and the stability of the membrane by confocal fluorescence microscopy. Figure 5A shows a confocal image of two polystyrene scaffolds: the control scaffold with no hole (2) and the nanofabricated scaffold with a single hole of surface area 300 nm × 300 nm (1). The hole was sealed with a lipid membrane. Under these conditions no fluorescence intensity inside the scaffolds was observed, indicating that the hole of the nanofabricated scaffold was effectively sealed by the lipid membrane and that the membrane has no defects or pores that could lead to passive diffusion of calcein into the scaffold. After the hole was sealed, the samples were kept at 4 °C for at least 2 weeks without showing any detectable diffusion of dye into the scaffolds. At the end of the experiments, the membrane was deliberately ruptured by the addition of 7 mM detergent (Triton X100) to the bulk solution immediately leading to calcein diffusion into the unloaded scaffold (Figure 5B), yielding a steplike increase in fluorescence intensity observed by fluorescence microscopy (Figure 5C). Approximately 80% of all addressed scaffolds were successfully sealed.

After successfully demonstrating that the holes can be sealed by membranes, we set out to build in control over permeability by embedding engineered MscL channel protein into the membranes. In its nonactivated state the pore of the MscL stays closed. However upon activation by specifically generating charge inside its hydrophobic pore, the pore starts to open and close continuously and allows the passage of molecules.[13,14] We activated MscL by adding 1 mM of [2-(trimethylammonio)ethyl]methanethiosulfonate (MTSET) to the bulk solution. MTSET is a positively charged compound that specifically binds to the free cysteine residues at the hydrophobic pore region of MscL. Insertion of MscL in the sealing membranes was achieved by reconstituting MscL into the liposomes by using the detergent-mediated reconstitution method prior to their collapse onto the hole.[23] The resulting 150 nm proteoliposomes were, then, used to generate giant unilamellar proteoliposomes by electroformation[24] (Supporting Information). Prior to the holes being sealed, a scaffold containing a single hole was loaded with PBS buffer and the bulk solution was perfused with ethanol-free buffer. Then the hole was sealed in a controlled fashion as before by using giant unilamellar proteoliposomes. Calcein was added to the bulk solution and properly sealed scaffolds were selected for monitoring MscL activity by CLSM. Prior to channel activation no calcein diffusion into the scaffold was observed. The seal remained intact for more than a day. However, the scaffolds became loaded with calcein as soon as the MscL channel was activated by the addition of MTSET to the bulk medium. Figure 6 shows the normalized fluorescence intensity in the sealed scaffold measured prior to and after activation of the MscL protein. The fluorescence intensity increased significantly after addition of the MTSET as a result of dye diffusion into the scaffold through the MscL channel as shown in Figure S2. As a control, scaffolds sealed with membrane devoid of MscL were incubated in calcein. No diffusion into the scaffold was observed after addition of MTSET until we deliberately ruptured the membrane by adding Triton X100 to the bulk solution.

After activation of the channels with MTSET, ∼10% of the fabricated scaffolds showed an increased fluorescence intensity, indicating that a large fraction of the scaffolds did not contain functional MscL channels. Clearly, the incorporation of functional MscL channels in the scaffolds is the limiting step in the overall success rate (currently ∼7%) in the fabrication of the biofunctionalized nanocontainers. Table S1 summarizes the yields of each individual step in the fabrication process.

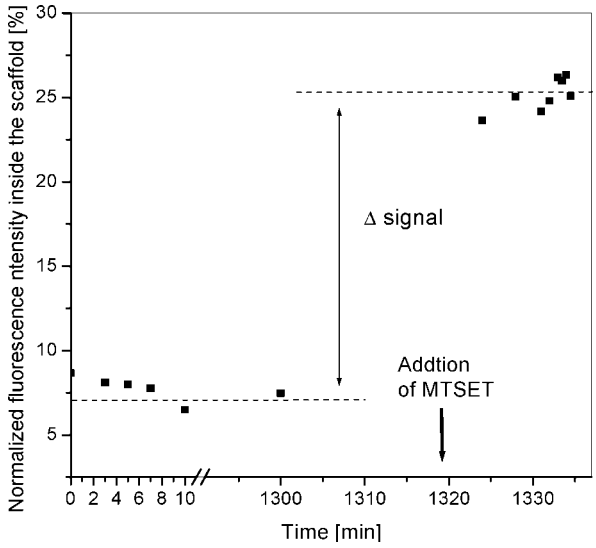

Figure 6. Fluorescence intensity inside the sealed scaffold normalized to the bulk fluorescence intensity prior to and after the activation of MscL channel protein upon addition of MTSET. Data points were obtained by averaging the fluorescence intensity inside the scaffold.

We have thus demonstrated, for the first time, a polymer–lipid hybrid nanocontainer with controlled permeability function. The nanocontainers consist of impermeable polymer scaffolds with nanofabricated holes sealed by lipid bilayers containing remotely actuatable pore forming channel proteins. This system allows exchange of solutions only after the channels are activated, hence forming large temporary pores in the hybrid container.

The controlled permeability of a nanocontainer opens new perspectives in studying single molecule interactions in confined biomimetic compartments. In such studies, it is important to specifically address the interior of the container, for example, to trigger or stop a reaction, to follow the reaction under different conditions, or to induce or investigate a conformational change of the encapsulated biomolecules. Until now, the most advanced systems included permanently opened channel pores in either liposomes or polymersomes or temporary temperature-triggered lipid-packing defects in liposomes.[3,4] In permanent channel-pore systems, the molecules smaller than the pore size are free to diffuse in and out of the system all the time. In the case of temperature-dependent temporary defects, the number of resulting pores in liposomes is not controllable and depends on the temperature of the environment, which may not always be convenient to change. However, in our system we can generate well-defined and stable temporary nanopores at will in both size and number, which allows different conditions inside and outside of the nanocontainer. The ability to exchange a solution and influence the environmental conditions independently could be particularly important for protecting encapsulated molecules from the outside or, in the case of nanoreactors, for the accumulation of the product inside the nanoreactor for a desired period of time.

A biohybrid nanocontainer is an ideal candidate for triggered delivery of drugs or imaging agents. It can possess properties such as controlled permeability, high temporal stability, flexibility to allow biofunctionalization, chemical surface modifications, and tuning of the scaffold properties. One of the major challenges in delivery systems is to have a stable container to prevent the leakage of the payload during its journey inside the body but a leaky container for instant release at the target site.[25] As containers, liposomes suffer from limited stability[26] and are leaky structures, whereas polymersomes are stable but do not allow instant release. In our hybrid system, polymer scaffolds form a robust architecture while a patch of sealed membrane serves as a natural environment for embedding pore-forming channel proteins and provides enough flexibility for the conformational changes that the channel requires to open a pore and release the payload. The exciting feature of this hybrid system as a triggered delivery device is that these pore-forming channels can be engineered in order to respond to the unique triggers necessary for release at the target delivery site.[27]

We thus believe that the addressable hybrid nanocontainer described here has potential applications in a broad variety of research areas, ranging from fundamental single molecule biophysics and biochemistry to targeted drug delivery and molecular imaging.

Acknowledgment. The authors thank Professor G. T. Robillard and Professor B. Poolman for critical reading of the manuscript. This project was financially supported by Biophysical Engineering Group (A.D., J.S.K., V.S.), BMTI Institute for Biomedical Technology, University of Twente (A.D., J.S.K., V.S.), NanoNed (A.K.), and The Netherlands Organization for Scientific Research (NWO-VIDI) (A.K.).

Supporting Information Available: The Materials and Methods section, an additional table summarizing the fabrication yields of the individual processing steps, additional figures showing an image of a hollow polystyrene scaffold containing two holes and images of a scaffold containing a single hole that is covered with a lipid membrane containing MscL channel protein. This material is available free of charge via the Internet at http://pubs.acs.org.

References

(1) Moerner, W. E. *Proc. Natl. Acad. Sci. U.S.A.* **2007**, *104*, 12596–12602.
(2) Boukobza, E.; Sonnenfeld, A.; Haran, G. *J. Phys. Chem. B* **2001**, *105*, 12165–12170.
(3) Cisse, I.; Okumus, B.; Joo, C.; Ha, T. *Proc. Natl. Acad. Sci. U.S.A.* **2007**, *104*, 12646–12650.
(4) Broz, P.; Driamov, S.; Ziegler, J.; Ben-Haim, N.; Marsch, S.; Meier, W.; Hunziker, P. *Nano Lett.* **2006**, *6*, 2349–2353.
(5) van den Bogaart, G.; Krasnikov, V.; Poolman, B. *Biophys. J.* **2007**, *92*, 1233–1240.
(6) Discher, D. E.; Eisenberg, A. *Science* **2002**, *297*, 967–973.
(7) Mayer, M.; Kriebel, J. K.; Tosteson, M. T.; Whitesides, G. M. *Biophys. J.* **2003**, *85*, 2684–2695.
(8) Drexler, J.; Steinem, C. *J. Phys. Chem. B* **2003**, *107*, 11245–11254.
(9) Römer, W.; Steinem, C. *Biophys. J.* **2004**, *86*, 955–965.
(10) Sukharev, S. I.; Blount, P.; Martinac, B.; Blattner, F. R.; Kung, C. *Nature* **1994**, *368*, 265–268.
(11) Perozo, E.; Kloda, A.; Cortes, D. M.; Martinac, B. *Nat. Struct. Biol.* **2002**, *9*, 696–703.
(12) Cruickshank, C. C.; Minchin, R. F.; Le Dain, A. C.; Martinac, B *Biophys. J.* **1997**, *73*, 1925–1931.
(13) Yoshimura, K.; Batiza, A.; Schroeder, M.; Blount, P.; Kung, C *Biophys. J.* **1999**, *77*, 1960–1972.

(14) Yoshimura, K.; Batiza, A.; Kung, C. *Biophys. J.* **2001**, *80*, 2198–2206.
(15) Koçer, A.; Walko, M.; Meijberg, W.; Feringa, B. *Science* **2005**, *309*, 755–758.
(16) Koçer, A.; Walko, M.; Bulten, E.; Halza, E.; Feringa, B. L.; Meijberg, W. *Angew. Chem., Int. Ed* **2006**, *45*, 3126–3130.
(17) Koçer, A.; Walko, M.; Feringa, B. L. *Nat. Protoc.* **2007**, *2*, 1426–1437.
(18) Orloff, J.; Utlaut, M.; Swanson, L. *High Resolution Focused Ion Beams: FIB and its Applications*; Kluwer Academic/Plenum Publishers: New York, 2003.
(19) Reyntjens, S.; Puers, R. *J. Micromech. Microeng.* **2001**, *11*, 287–300.
(20) Woldering, L. A.; Otter, A. M.; Husken, B. H.; Vos, W. L. *Nanotechnology* **2006**, *17*, 5717–5721.
(21) Beach, E.; Keefe, M.; Heeschen, W.; Rothe, D. *Polymer* **2005**, *46*, 11195–11197.
(22) Monahan, J.; Gewirth, A. A.; Nuzzo, R. G. *Anal. Chem.* **2001**, *73*, 3193–3197.
(23) Rigaud, J-L.; Pitard, B.; Levy, D. *Biochim. Biophys. Acta* **1995**, *1231*, 223–246.
(24) Girard, P.; Pécréaux, J.; Lenoir, G.; Falson, P.; Rigaud, J-L.; Bassereau, P. *Biophys. J.* **2004**, *87*, 419–429.
(25) Sandström, M. C.; Ickenstein, L. M.; Mayer, L. D.; Edwards, K. *J. Controlled Release* **2005**, *107*, 131–142.
(26) Lee, J. C. M.; Bermudez, H.; Discher, B. M.; Sheehan, M. A.; Won, Y. Y.; Bates, F. S.; Discher, D. E. *Biotechnol. Bioeng.* **2001**, *73*, 135–145.
(27) Kocer, A. *J. Liposome Res.* **2007**, *17*, 219–225.

NL073211B